

Biomedical Physics & Engineering Express



PAPER

Non-conventional deep brain stimulation in a network model of movement disorders

OPEN ACCESS

RECEIVED

24 April 2024

REVISED

27 November 2024

ACCEPTED FOR PUBLICATION

10 December 2024

PUBLISHED

20 December 2024

Nada Yousif¹ , Peter G Bain^{2,3} , Dipankar Nandi^{2,3} and Roman Borisyuk⁴ ¹ School of Physics, Engineering and Computer Science, University of Hertfordshire, United Kingdom² Department of Brain Sciences, Imperial College London, United Kingdom³ Imperial College Healthcare NHS Trust, United Kingdom⁴ Department of Mathematics and Statistics, University of Exeter, United KingdomE-mail: n.yousif@herts.ac.uk**Keywords:** deep brain stimulation, movement disorders, genetic algorithm, network model

Original content from this work may be used under the terms of the [Creative Commons Attribution 4.0 licence](https://creativecommons.org/licenses/by/4.0/).

Any further distribution of this work must maintain attribution to the author(s) and the title of the work, journal citation and DOI.

**Abstract**

Conventional deep brain stimulation (DBS) for movement disorders is a well-established clinical treatment. Over the last few decades, over 200,000 people have been treated by DBS worldwide for several neurological conditions, including Parkinson's disease and Essential Tremor. DBS involves implanting electrodes into disorder-specific targets in the brain and applying an electric current. Although the hardware has developed in recent years, the clinically used stimulation pattern has remained as a regular frequency square pulse. Recent studies have suggested that phase-locking, coordinated reset or irregular patterns may be as or more effective at desynchronising the pathological neural activity. Such studies have shown efficacy using detailed neuron models or highly simplified networks and considered one frequency band. We previously described a population level model which generates oscillatory activity in both the beta band (20 Hz) and the tremor band (4 Hz). Here we use this model to look at the impact of applying regular, irregular and phase dependent bursts of stimulation, and show how this influences both tremor- and beta-band activity. We found that bursts are as or more effective at suppressing the pathological oscillations compared to continuous DBS. Importantly however, at higher amplitudes we found that the stimulus drove the network activity, as seen previously. Strikingly, this suppression was most apparent for the tremor band oscillations, with beta band pathological activity being more resistant to the burst stimulation compared to continuous, conventional DBS. Furthermore, our simulations showed that phase-locked bursts of stimulation did not convey much improvement on regular bursts of oscillation. Using a genetic algorithm optimisation approach to find the best stimulation parameters for regular, irregular and phase-locked bursts, we confirmed that tremor band oscillations could be more readily suppressed. Our results allow exploration of stimulation mechanisms at the network level to formulate testable predictions regarding parameter settings in DBS.

Abbreviations

DBS	Deep brain stimulation		given level of population activity $x(t)$.
VIM	Ventral intermediate nucleus	τ_i	Time constant of the change over time in the proportion of cells firing in a population j .
STN	Subthalamic nucleus		
GPe	Globus Pallidus externa	E_e and I_i	Represents the number of active neurons in an excitatory (e) or inhibitory (i) population.
GPI	Globus Pallidus interna		
ET	Essential tremor		
PD	Parkinson's disease		
$Z_j(x)$	The proportion of cells firing in population j for a	w_n	The strength of the connection between two

	populations, where $n = 1, 2 \dots 11$.
ext	A constant ascending external input to the DCN population.
$b_e, b_i, \theta_e, \theta_i$	Constants defined by Wilson and Cowan (1972).
k_e and k_i	The maximum values of the response functions for excitatory and inhibitory populations.

1. Introduction

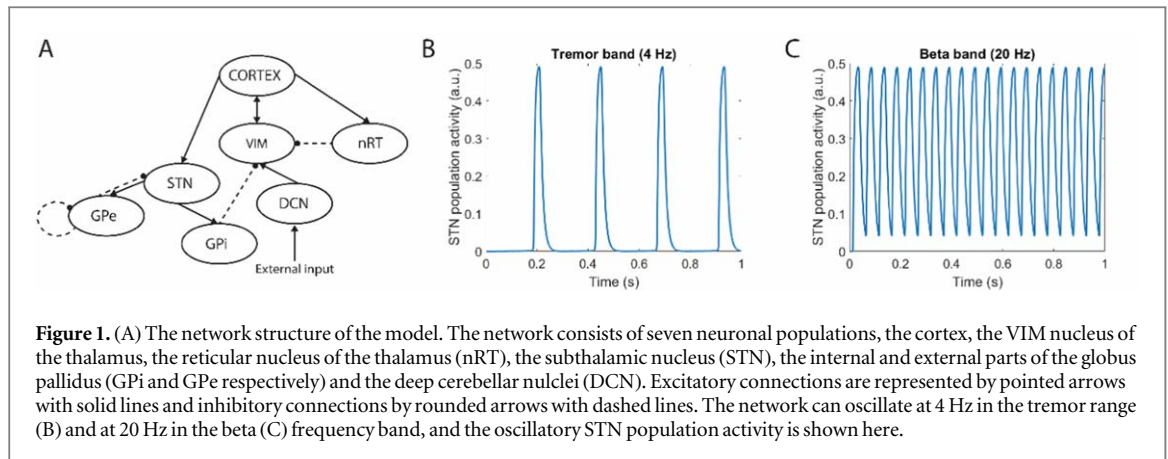
Movement disorders such as Parkinson's disease (PD) and essential tremor (ET) affect up to 6% of people over the age of 60 (Louis and Ferreira 2010, Tysnes and Storstein 2017) and impact significantly on family members, carers and the health service. One well-established surgical treatment is deep brain stimulation (DBS) which has treated over 200,000 people worldwide over the last few decades for several neurological conditions including PD and ET (Vedam-Mai *et al* 2021). The procedure involves implanting electrodes into disorder-specific targets in the brain and applying electrical stimulation (Benabid *et al* 1987). For many years, the electrodes consisted of four cylindrical contacts, but more recently this design has been evolving to include electrodes with varying numbers of contacts and varying shapes of contacts, through which the stimulation can be applied (Potel *et al* 2022). This has allowed for more flexibility, and the exploration of more complex stimulation protocols.

Conversely, since its inception the stimulation pattern used for DBS has consisted of a regular square wave, with specific parameters that can be varied: frequency, pulse width and amplitude (Kuncel and Grill 2004). This affords the clinician some degree of flexibility, and yet there is a narrow window within which to vary these parameters. This is due to the optimal clinical effect being obtained with specific frequencies, a reluctance to use high energy parameters to conserve battery life, and the need to avoid inducing side effects (Yousif *et al* 2012). However, in recent years there has been a focus on investigating novel stimulation patterns which achieve clinical improvement in symptoms and minimise energy consumption and side effects (Koeglsperger *et al* 2019; Daria Bogdan *et al* 2020). The mechanism of action of DBS remains unclear and a topic of discussion in the literature. Given the similar outcome achieved by DBS as by lesioning, DBS has been referred to a functional lesion and discussion often centres on whether DBS simply excites or inhibits neuronal activity. More recently, it is thought that DBS triggers a variety of mechanisms through which functional improvements are seen in patients (Kringelbach *et al* 2007), from immediate

effects such as depolarisation of neuronal membranes, to long term effects such as neural repair (Pei *et al* 2024). One hypothesis is that pathological oscillatory activity is desynchronised by the applied stimulation (Rubin and Terman 2004, McIntyre and Hahn 2010, Yousif *et al* 2017, 2020). The origin for such pathological activity is not fully understood, though previous work has shown the importance of the connection between the cortex and subthalamic nucleus (Litvak *et al* 2011) and more recently the globus pallidus (Crompe *et al* 2020). Recently, it has been suggested that changes in synaptic connectivity within populations occur as a result of plasticity mechanisms, which may also lead to pathological activity in Parkinson's disease (Chu *et al* 2015, 2017, Madadi Asl *et al* 2022).

Recent computational modelling studies have suggested that phase-locking, coordinated reset (Popovich *et al* 2006, Hauptmann and Tass 2007, Tass *et al* 2012) or irregular patterns may be as or more effective at desynchronising the pathological neural activity. Conversely, an early study showed that irregularity in the DBS stimulus did not improve desynchronization of a basal ganglia network (Dorval *et al* 2010), however they used irregular single pulses. Similarly, Summerston *et al* (2015) looked at the impact of irregularity added to single pulses and showed that this did not change the overall firing rate in networks but did change the entropy. More recently, studies have considered temporally irregular bursts of stimuli (Santos-Valencia *et al* 2019), and shown that in a model of epilepsy this slows seizure onset. Furthermore, Duchet *et al* (2021) showed that rather than irregular bursts, phase-locked bursts can improve desynchronization in network models of tremor. These and other studies have mainly focussed on detailed biophysical models or highly simplified networks and considered how the stimuli desynchronise the pathological activity in a single frequency range (Brocker *et al* 2013, Holt *et al* 2016, Toth and Wilson 2022). Furthermore, the converse has also been shown, i.e. that stimuli trains with bursts do not confer any improvement in suppression of symptoms over regular stimulation (Birdno *et al* 2012). More recent work suggests that when synaptic plasticity mechanisms come into play, the impact of burst and regular stimulation are more similar (Madadi *et al* 2023).

In this study we investigate how such non-conventional burst stimulation impact the dynamics of our previously presented, anatomically realistic network model. This model generates oscillatory activity in both the beta frequency band (20 Hz), which has been linked to Parkinson's disease, and oscillations in the tremor frequency range (4 Hz). We used this model to explore the parameter space and separated regions with the dynamics associated with these different frequencies, also describing how the network transitioned between the different oscillatory states and how DBS changed the two types of pathological oscillations. In this study, we use this same model to look at



the impact of applying regular, irregular and phase dependent burst stimulation on this network behaviour. We show how, with the use of an optimisation approach using genetic algorithm, we can find parameters to define novel stimulation paradigms which suppress the different pathological activity at the network level.

2. Materials and methods

We used our population representation of the thalamocortical basal ganglia-cerebellar network (Merrison-Hort *et al* 2013, Yousif *et al* 2017, 2020), which includes: a cortical population, a cerebellar population, two thalamic populations, plus a basal ganglia part including the subthalamic nucleus (STN), the external part of the globus pallidus (GPe) and the internal part of the globus pallidus (GPi) (figure 1(A)). The network includes known connections between the populations, such as the cortical drive to the STN, the hyper-direct pathway, and an inhibitory output from the basal ganglia to the thalamus. The network receives a constant ascending drive via the cerebellar population to the thalamus. As shown in a recent review of the ‘Cortico-Basal Ganglia-Cerebellar Network’ (Milardi *et al* 2019) our knowledge of the connections between these structures is constantly being updated due to new research, beyond the traditional image of the direct and indirect pathways. Our model includes many of these structures and known connections and focusses on combining the simple STN-GPe recurrent network, with a thalamocortical network and including the cerebellar input. Although, as with all models, it is a simplification of the full biological picture, it captures these important pathways and the hyper-direct pathway thought to be central to voluntary movement (Nambu, Tokuno and Takada 2002).

The Wilson-Cowan approach was used to model the network (Wilson and Cowan 1972), which assumes that neurons within a population are in close spatial proximity, ignores spatial interactions and only represents temporal dynamics. The activity of each

population is represented by the proportion of cells which are firing action potentials per unit time. As presented previously, the network consists of an excitatory cortical population (Cx below), two thalamic populations, the excitatory ventral intermediate (VIM) nucleus and the inhibitory reticular nucleus (nRT), an excitatory population of deep cerebellar nuclei neurons (DCN), an excitatory population representing the STN, and two inhibitory populations representing the GPe and the GPi. The network structure can be seen in figure 1(A). Hence, the model consists of seven first-order coupled differential equations, shown below:

$$\tau_{Cx} \frac{dE_{Cx}}{dt} = -E_{Cx} + (k_e - E_{Cx}(t)) \cdot Z_e(w_1 E_{VIM}(t)) \quad (1)$$

$$\tau_{VIM} \frac{dE_{VIM}}{dt} = -E_{VIM} + (k_e - E_{VIM}(t)) \cdot Z_e(w_2 E_{Cx}(t) - w_3 I_{nRT}(t) + w_4 E_{DCN}(t) - w_5 I_{GPi}(t)) \quad (2)$$

$$\tau_{nRT} \frac{dI_{nRT}}{dt} = -I_{nRT} + (k_i - I_{nRT}(t)) \cdot Z_i(w_6 E_{Cx}(t)) \quad (3)$$

$$\tau_{DCN} \frac{dE_{DCN}}{dt} = -E_{DCN} + (k_e - E_{DCN}(t)) \cdot Z_e(ext) \quad (4)$$

$$\tau_{GPe} \frac{dI_{GPe}}{dt} = -I_{GPe} + (k_i - I_{GPe}(t)) \cdot Z_i(w_7 E_{STN}(t) - w_8 I_{GPe}(t)) \quad (5)$$

$$\tau_{GPi} \frac{dI_{GPi}}{dt} = -I_{GPi} + (k_i - I_{GPi}(t)) \cdot Z_i(w_9 E_{STN}(t)) \quad (6)$$

$$\tau_{STN} \frac{dE_{STN}}{dt} = -E_{STN} + (k_e - E_{STN}(t)) \cdot Z_e(w_{10} E_{Cx}(t) - w_{11} I_{GPe}(t)) \quad (7)$$

Here, the functions E_e ($e = Cx, VIM, DCN$ or STN) and I_i ($i = nRT, GPe$ or GPi) represent the number of active neurons in the relevant excitatory or inhibitory population at a given time. The strength of the connection between two populations is given by a weight parameter w_n , where $n = 1, 2, \dots, 11$. The value of this weight represents the product of the average

Table 1. The 11 connection weights as shown in equations (1) to (7) are given here for the two oscillatory pathological states explored in the manuscript. The set of parameters for achieving the healthy state, which served as our baseline for the optimisation is also given in the table.

Weight	Healthy state	Tremor band	Beta band
w1	20	20	20
w2	5	12	5
w3	8	8	8
w4	25	9	20
w5	15	15	15
w6	5	5	5
w7	19	5	5
w8	5	5	5
w9	15	15	15
w10	20	20	20
w11	20	20	20
ext	3.42	3.42	3.42

number of contacts per cell and the average postsynaptic current induced in the postsynaptic cell by a presynaptic action potential. Note that in equation (4), which represents the DCN population, the activity is independent of the dynamics of the other populations, and only provides an input into the VIM population. Therefore, in this model, the DCN population will tend to a stationary value and not oscillate. Furthermore, the DCN receives a constant input representing an ascending external input (ext) which drives the network. All weight parameters, and the value of the ‘ext’ parameter, are given in table 1. We used two sets of weights, one which resulted in the network oscillating with a frequency in the tremor band (figure 1(B)) and one set which resulted in beta band frequency oscillations (figure 1(C)). These weights were defined in our previous study (Yousif et al 2020).

The functions $Z_e(x)$ and $Z_i(x)$ represent the proportion of cells firing in an excitatory (e) or inhibitory (i) population for a given level of average membrane potential activity $x(t)$. Previously these functions were derived by assuming that the population has a distribution of neural thresholds and that all cells in the population have the same average level of membrane potential activity (Wilson and Cowan 1972). Another approach can be to assume that the neurons within a population have the same threshold but varying numbers of afferent synapses. Either approach results in response functions that are monotonically increasing sigmoid functions, as shown here:

$$Z_p(x) = \frac{1}{1 + \exp(-b_p(x - \theta_p))} - \frac{1}{1 + \exp(b_p \theta_p)} \quad (8)$$

where p represents e or i, b_p and θ_p are constants, and x is the level of input activity. We use the parameters given by Wilson and Cowan: $\theta_e = 1.3$, $b_e = 4$, $\theta_i = 2.0$, and $b_i = 3.7$. The maximum values of these response functions are given by the parameters k_e and k_i , where $k_e = 0.9945$ and $k_i = 0.9994$. The parameters τ_e and τ_i represent the time constant of the change over time in

the proportion of non-refractory cells which are firing in a population, in response to the change over time in the average membrane potential activity of the cells. This is typically set to be equal to the membrane time constant of the cells in the population, and normally in the range 10–20 ms (Denham and Borisyuk 2000). Here, all time constants were set to 10 ms and unchanged for all simulations as in our previous work.

2.1. DBS input

We simulated regular DBS of the network via the application of a high frequency input to the GPe, STN or thalamus by modelling a simple square pulse. An example square pulse is shown in figure 2 inset. In this example, the frequency is set at 10 Hz, therefore the period of the function will be 100 ms. The square pulse has a value of one for half of the period i.e. 50 ms, and zero for the other half. For the square pulses used in this study, we kept the frequency set to 100 Hz, which is a therapeutic value used for DBS (Kuncel and Grill 2004), and varied the amplitude of the square pulse to between one and 10 arbitrary units (a.u.).

This change results in an additional term in the equation for the stimulated population, for example, the STN equation changed as follows:

$$\tau_{STN} \frac{dE_{STN}}{dt} = -E_{STN} + (k_e - E_{STN}(t)) \cdot Z_e(w_{10}E_{STN}(t) - w_{11}I_{GPe}(t) + DBS(t)) \quad (9)$$

For bursts of stimulation, we used the same square wave as above, but used onset times and durations to limit the square wave into bursts (figure 2). We used three different inter-burst frequencies, and each had an associated duration, as summarised in table 2. To make our regular bursts irregular, we added random noise to the onset time of each burst, resulting in the same number of bursts, but occurring randomly (figure 2). The noise was added as pseudorandom values between zero and one to the burst onset times and drawn from the standard uniform distribution via the Matlab function ‘rand’. For phase-locked bursts, first the peak times of the network oscillations were found. We then ran five different simulations, with the bursts of stimulation being applied coincident with the peaks of the oscillations, the peaks plus or minus half of the cycle time period and the peaks plus or minus a quarter of the time period.

2.2. Numerical details and analysis

As in our previous study, all simulations were run in Matlab via custom written scripts. We used ‘ode23tb’ to numerically integrate the set of differential equations. We simulated the network for 1.1 s using a time step of 0.1 ms. We found that the length of the simulation did not affect the network activity, as the frequency and range of the activity was unchanged if the simulation lasted 1 s or 10 s. We discarded the first 0.1 s to allow the network to settle. We tested network activity with all populations starting at zero activity

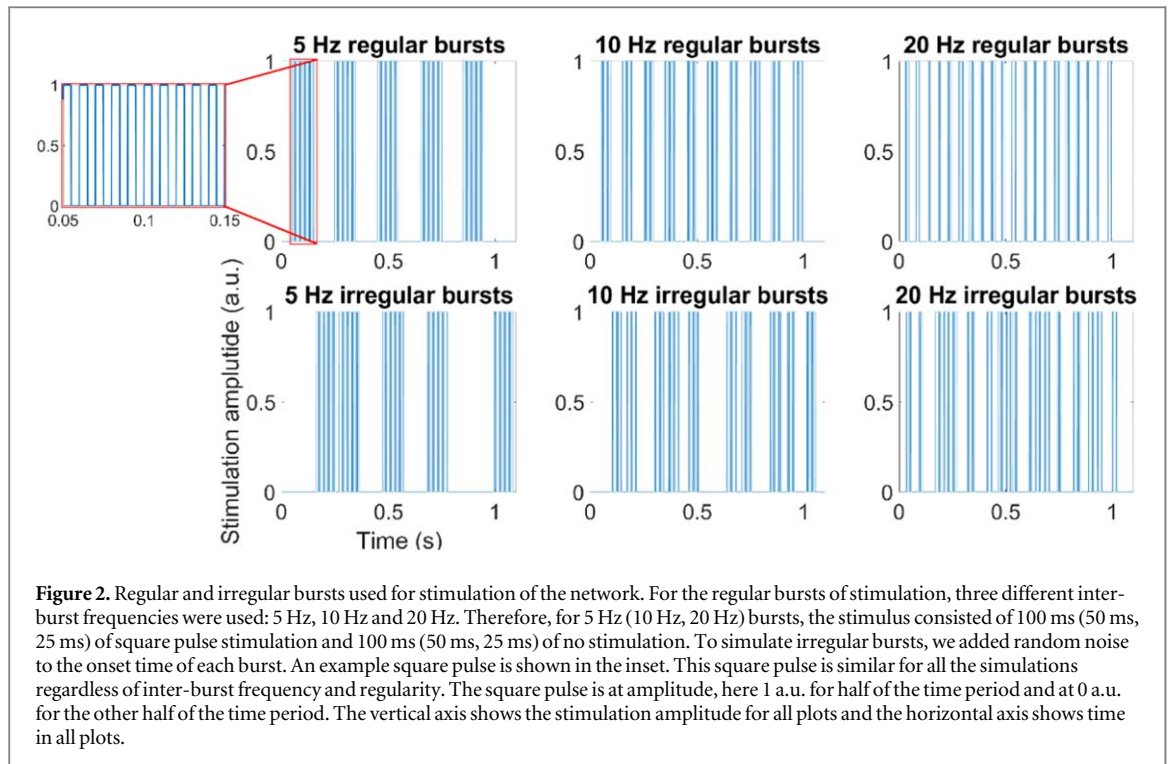


Table 2. The parameters used for the different burst stimulation. The burst stimulation is delivered as a regular train of bursts with a specified burst frequency and burst duration. We also apply irregular trains of bursts, which are the same as the regular bursts but with random noise added to the onset times of the bursts. The table also shows the range used for this added noise. Finally, we simulated phase-locked stimulation. The table shows the five phase shifts we used, 0 shift, or stimulation bursts delivered at the same time as the peak of the oscillation, $\pm \frac{1}{2}$ cycle or bursts delivered at \pm half the period away from the peaks of the oscillation and $\pm \frac{1}{4}$ cycle or bursts delivered at \pm quarter of the period away from the peaks of the oscillation.

Type	Inter-burst frequency	Pulse duration	Noise range	Phase shift
Regular and irregular	5 Hz	100 ms	0–200 ms	n/a
Regular and irregular	10 Hz	50 ms	0–100 ms	n/a
Regular and irregular	20 Hz	25 ms	0–50 ms	n/a
Phase locked	4 Hz	100 ms	n/a	At peak, $\pm \frac{1}{2}$ cycle, $\pm \frac{1}{4}$ cycle
Phase locked	20 Hz	25 ms	n/a	At peak, $\pm \frac{1}{2}$ cycle, $\pm \frac{1}{4}$ cycle

and with random activity, but this did not affect the frequency of the network activity. Therefore, we ran all simulations with zero initial conditions for consistency across, as the phase locked stimuli require known oscillation peak times. As we showed in our previous work (Yousif *et al* 2020), the pathological tremor band and beta band activity was seen in all populations, except the DCN. Therefore, in this study we show the STN activity to demonstrate the impact of stimulation on the network. To quantify the impact of the stimuli on the network, we measured the range, defined as the maximum minus the minimum of the STN activity over the entire simulation time, discarding the first 0.1 ms. Therefore, if the population activity is constant the range would be equal to zero, but if the activity is oscillatory, the range would equal the amplitude of the oscillation.

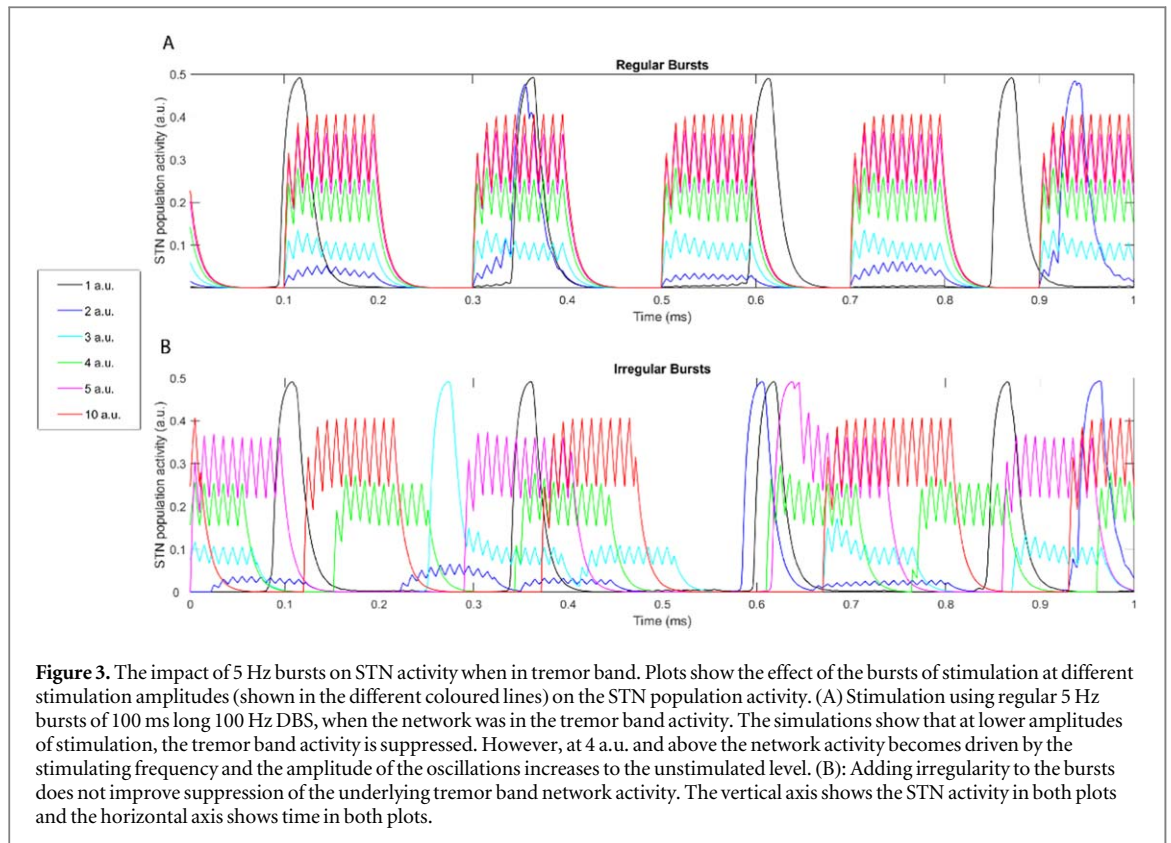
2.3. Optimisation of stimulation parameters

To ensure that we found parameters to abolish the unwanted oscillations, we used a genetic algorithm to

optimise the stimulus parameters (Li *et al* 2021). Genetic algorithms are an optimisation approach which allow the parameter space to be searched and an objective function to be minimised by changing a population of solutions to a problem. We followed an approach presented by Li *et al* (2021), using the ‘ga’ function in MATLAB. This function allows the parameters of interest to be limited by a minimum and a maximum. We estimated the optimal values for the amplitude, frequency, and pulse duration parameters. The first two were constrained by the typical range of these parameters used clinically (table 3) and the pulse duration based on our initial simulations with the model. The noise parameter, which shifted the onset of the irregular bursts, was set as pseudorandom values between zero and double the pulse duration. The objective function was the cross-correlation between the Fourier transform of the network activity and the network activity in the gamma band which we previously proposed represents healthy network behaviour (Yousif *et al* 2020). We set the initial tolerance to

Table 3. The parameters used for the genetic algorithm. The table shows the minimum and maximum of the three parameters that were used for the objective function and the noise for the irregular bursts was calculated as twice the pulse duration.

Type	Maximum generations	Tolerance	Amplitude	Frequency	Pulse duration	Noise
Regular	Standard: 128	Standard: 1×10^{-3}	Standard: 0.5–5 a.u.	Standard: 100–200 Hz	10–300 ms	n/a
Irregular		Additional: 1×10^{-9}	Additional: 0.5–15 a.u.	Additional: 100–300 Hz		0—twice the pulse duration
Phase-locked						No noise, bursts locked to peak



0.001 and the maximum number of generations was to 128, but we also explored the impact of changing these options when we did not obtain good suppression of oscillatory activity with the standard set of parameters.

3. Results

3.1. Tremor band suppression

We first examined the impact of regular burst DBS and irregular burst DBS on the tremor band activity in the model. We stimulated the model using regular bursts with 100 Hz within burst frequency and 5 Hz inter-burst frequency. Interestingly, we found suppression of the tremor band network activity at amplitudes greater than 3 a.u. with regular bursts (figure 3(A)). However, as the amplitude of stimulation increased, the network activity was driven by the stimulation and increases in amplitude. This predicts that for intermittent or burst type stimulation, low amplitudes may be preferred. Interestingly, adding noise to the onset times of the bursts to create irregular bursting stimulation (figure 3(B)), did not improve suppression of the oscillatory activity.

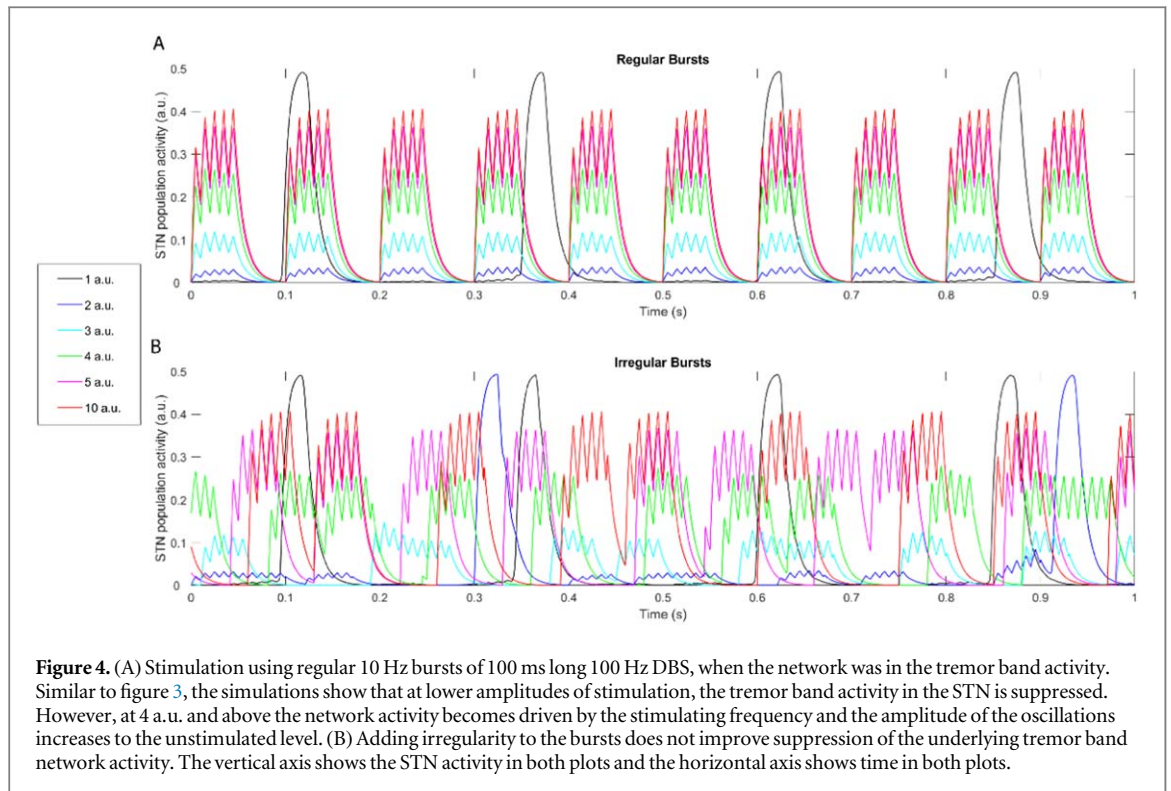
Increasing the inter-burst frequency to 10 Hz, also achieved suppression of the tremor band network activity. Figure 4 shows that this suppression could be achieved with amplitudes greater than 2 a.u., and therefore better suppression was achieved. Once again, increasing the amplitude of the stimulation lead to the network being driven by the high frequency stimulus. However, unlike the 5 Hz bursts, the addition of the irregularity in the burst onsets appears to confer some

improvement in suppression, as not all bursts drive the network response. This appears to occur when the bursts arrive close to one another. Finally, we applied bursts with a frequency of 20 Hz, and the results were similar to the 5 and 10 Hz burst stimulation. We quantified our simulations using the range of the STN activity, and the results are shown in figure 5. Comparing the impact of regular DBS in figure 5(A) to regular burst stimulation at different frequencies and amplitudes on tremor band activity (dotted lines) in figure 5(B) clearly indicates that regular bursts reduce the amplitude of the STN oscillation at 2 and 3 a.u. but this effect vanishes at higher amplitudes.

Finally, we considered applying the burst stimulation in a phase locked manner. Bursts were applied at the peak of the network activity, at $\pm \frac{1}{2}$ a cycle and at $\pm \frac{1}{4}$ a cycle. when oscillating with the tremor band frequency, the impact of the phase-locked bursts was similar to the regular bursts when the stimulation preceded the peak of oscillation (figure 5).

3.2. Beta band suppression

Next, we applied burst DBS and irregular burst DBS on the network when in the beta band range. Using regular bursts with a 100 Hz frequency and a 5 Hz inter-burst frequency. In this case, we found limited suppression of the beta band network activity at amplitudes greater than 4 a.u., with regular bursts. However, as the amplitude of stimulation increased, the network activity became driven by the stimulation and increased in amplitude. Interestingly, adding noise to the onset times of the bursts to create irregular bursting stimulation, did not improve the suppression



achieved by stimulation. Increasing the inter-burst frequency to 10 Hz, also achieved only partial suppression of the network activity, but only during the bursts of stimulation. Most interestingly, when we applied regular bursts with a frequency of 20 Hz, there is almost no change to the beta band activity. When irregularity is added to the onset of the burst stimulation, some suppression is seen, though once again the beta activity is not completely suppressed. The quantification of our simulations can be seen in figure 5. This time, comparing the impact of burst stimulation at different frequencies and amplitudes on beta band activity (dashed lines) in figures 5(B) and (C) to regular DBS in figure 5(A) shows very little impact of stimulation on the amplitude of the STN oscillation. This contrasts with the regular DBS (figure 5(A)) which does reduce the beta band activity at 4 a.u. and above. Finally, the phase locked bursts had little effect on the underlying network activity (figure 5(D)).

3.3. GPe stimulation

In striking contrast to STN stimulation, we also show the impact of the different stimulation patterns when applied to the GPe. We quantified this using the same measure of the range of the STN activity (figure 6). Comparing the impact of burst stimulation at different frequencies and amplitudes to regular DBS in figure 6(A) clearly indicates that most types of the burst stimulation are ineffective at reducing the amplitude of the STN oscillations (figures 6(B) and (C)). This is apart from the phase locked stimulation for stimuli preceding the peak of the oscillation, but only on when the network is oscillating in the tremor band (figure 6(D)).

3.4. Optimisation

We ran the genetic algorithm for the regular, irregular and bursts locked to the peak of the unwanted oscillations, with the network in the tremor and the beta band states. Table 4 shows the results for the six options. In all cases except the regular bursts for the tremor band activity, the optimisation was run with the 'additional' set of parameters from table 3 as well as the standard to check if a better fit could be obtained. With the standard parameters, the optimal frequency found was greater than the 100 Hz used in our exploratory simulations, and the amplitude was typically on the order of 5 a.u. The duration varied from a minimal 10 ms burst to a much longer 263 ms burst. The additional parameters were only used for two cases, regular and irregular bursts in the beta band.

Figure 7 shows the impact of the burst stimulation on the network activity when the optimised parameters are used for each condition, compared to the unstimulated cases in each oscillatory state (figures 7(A) and (E)). Interestingly, the algorithm was able to find an optimal solution for suppressing tremor band oscillations in all cases, and the beta band activity in one of the three cases. The tremor band oscillation appears to be best suppressed by regular bursts with parameters of 2.08 a.u. amplitude, 199 Hz frequency and 12 ms duration or 43 Hz inter-burst frequency (figure 7(B)), which was consistent with our initial exploration. Tremor band activity was also well suppressed with irregular (figure 7(C)) and phase locked bursts (figure 7(D)). Once again, we found that though beta band oscillations were partially suppressed by regular (figure 7(F)) and irregular bursts (figure 7(G)), this only occurred during the burst itself.

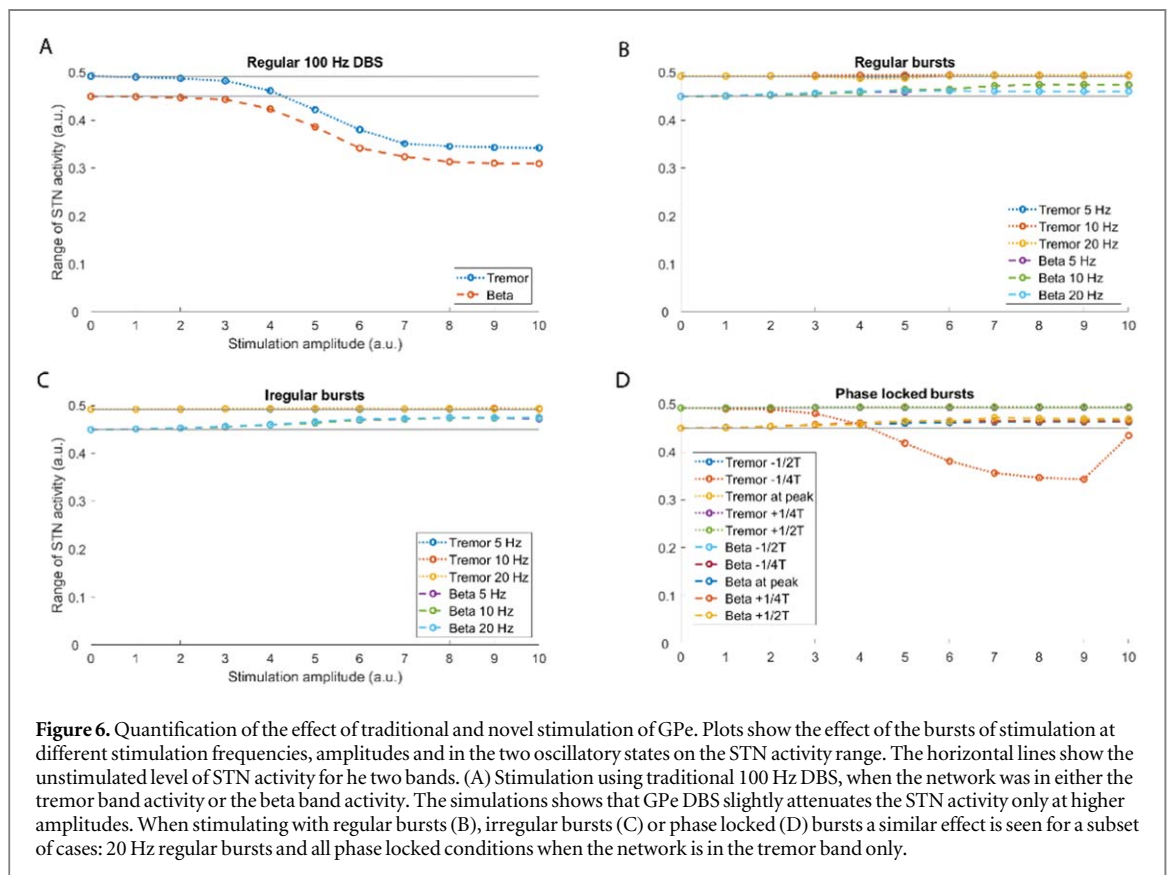
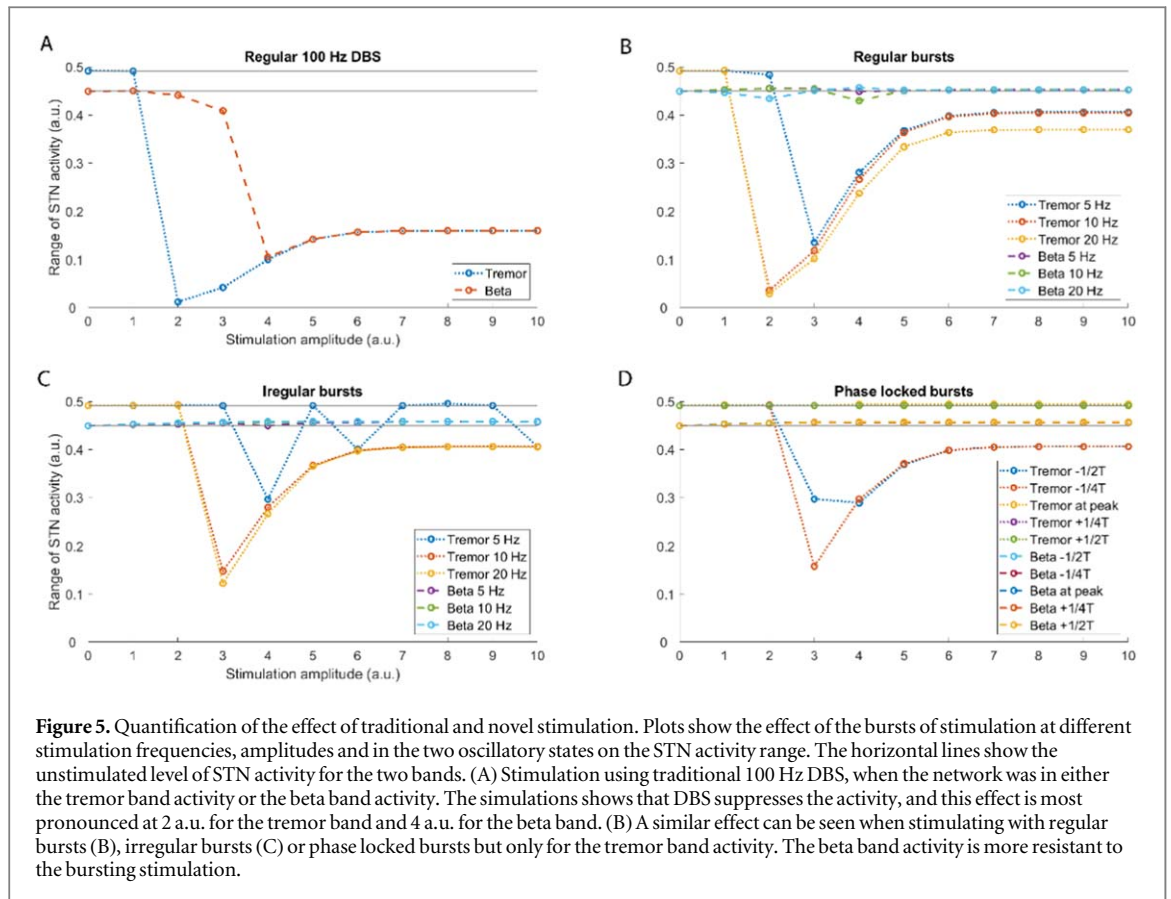


Table 4. Results from the optimisation. The table shows the parameters identified by the algorithm for suppression of the tremor and beta band oscillations by regular bursts, irregular bursts and bursts phase-locked to the peak of the pathological oscillation. In cases where the additional optimisations were attempted both sets of parameters are shown.

Mode	Burst type	Options	Amplitude (a.u.)	Frequency (Hz)	Pulse duration (ms)
Tremor	Regular	Standard	2.08	199	12
Beta	Regular	Standard	5.00	197	53
		Additional	11.5	279	217
Tremor	Irregular	Standard	4.49	187	10
Beta	Irregular	Standard	4.97	200	201
		Additional	9.34	296	298
Tremor	Phase-locked to peak	Standard	5.00	192	263
Beta	Phase-locked to peak	Standard	4.97	199	92

Remarkably however, the results show that the phase locking of bursts can be very effective at suppressing the unwanted oscillations in the beta band when using the optimised parameters of 5.00 a.u. amplitude, 199 Hz frequency and 92 ms duration or 5 Hz inter-burst frequency (figure 7(H)).

4. Discussion

We used our previously presented population model of the thalamocortical basal ganglia-cerebellar network (Yousif *et al* 2020) to investigate the effects of bursting deep brain stimulation patterns on dynamics. Our network represents synchronised activity both in the tremor band frequency range thought to be pathological in essential tremor (Deuschl, Bain and Brin 1998) and in the beta band range, thought to be elevated in Parkinson's disease (Little and Brown 2014). We previously showed the impact of standard, regular DBS on these two oscillatory states and found that such DBS could switch the activity from high-amplitude pathological oscillations to low-amplitude, high-frequency activity (Yousif *et al* 2017, 2020). Our model is consistent with previous rate models of this network (Leblois *et al* 2006, van Albada *et al* 2009), which also probe the generation of oscillations arising from the dynamics in the basal ganglia, thalamocortical connections.

In this study, we extended this work to look at regular bursts of DBS at different amplitudes and frequencies; irregular bursts at different amplitudes and frequencies; and phase locked bursts at different amplitudes and phase shifts. Previous studies have shown conflicting impact of such burst stimulation yet only few studies have considered the impact on the network dynamics (e.g. Duchet *et al* 2020). Interestingly, we found variable effects of burst stimulation depending on the network state. When the network was oscillating in the tremor band, we found that 5 Hz bursts of DBS were not as effective at suppressing the tremor band compared to continuous DBS. This was evident as the amplitude required to fully suppress the tremor band activity was increased (starting at 3 a.u.) compared to in our previous study (started at 2 a.u.). However, better suppression was

achieved with an inter burst frequency of 10 Hz (~double the tremor), where the amplitude at which suppression occurred matched the continuous DBS amplitude. Surprisingly, 20 Hz bursts was sub-optimal compared to continuous DBS. In all cases, adding irregularity did not appear to improve the suppression.

These results are in line with previous studies showing that continuous DBS out-performs irregular DBS (Dorval *et al* 2010; Oza *et al* 2018). On the other hand, this is in contrast with other research which show that adding irregularity can achieve good desynchronization, some of which have also shown experimental proof (Zeitler and Tass 2018, Khaledi-Nasab, Kromer and Tass 2021a, 2021b, Pfeifer *et al* 2021). Such differences could be due to the simplicity of the model presented here. However, as we have discussed in our previous work, this simplicity is intrinsic when consider the dynamics of the network in absence of detailed physiological properties. In our model, we found that phase-locked stimulation offers no improvement on tremor band suppression compared to either continuous DBS or 10 Hz bursts of DBS. This could be an effect related to the frequency of bursts, rather than the relationship of the bursts to the pathological network activity, as in the phase locked scheme, the network was stimulated by 4 Hz inter-burst frequency. Importantly, we further observed that as the amplitude of stimulation increases, the network activity becomes driven by the stimulus. This could represent a limitation of the model, but we should also consider amplitude dependence when investigating the use of bursts of DBS pulses.

A study by Brocker *et al* (2013) trialled non-regular DBS in patients with Parkinson's, and its effect on both motor performance and the beta band. Interestingly, in this paper the authors discuss that random DBS in patients with ET is less effective at dampening their tremor as 'long gaps in the stimulation train allow pathological activity to propagate through the stimulated nucleus'. We observed a similar result, with the oscillations in the beta band more than with those in the tremor band. Brocker *et al* (2013) showed that in PD, irregular stimulation did improve the participants' ability in a motor task of finger tapping. Their computational model further showed that such irregular DBS dampened beta synchrony. However, it is

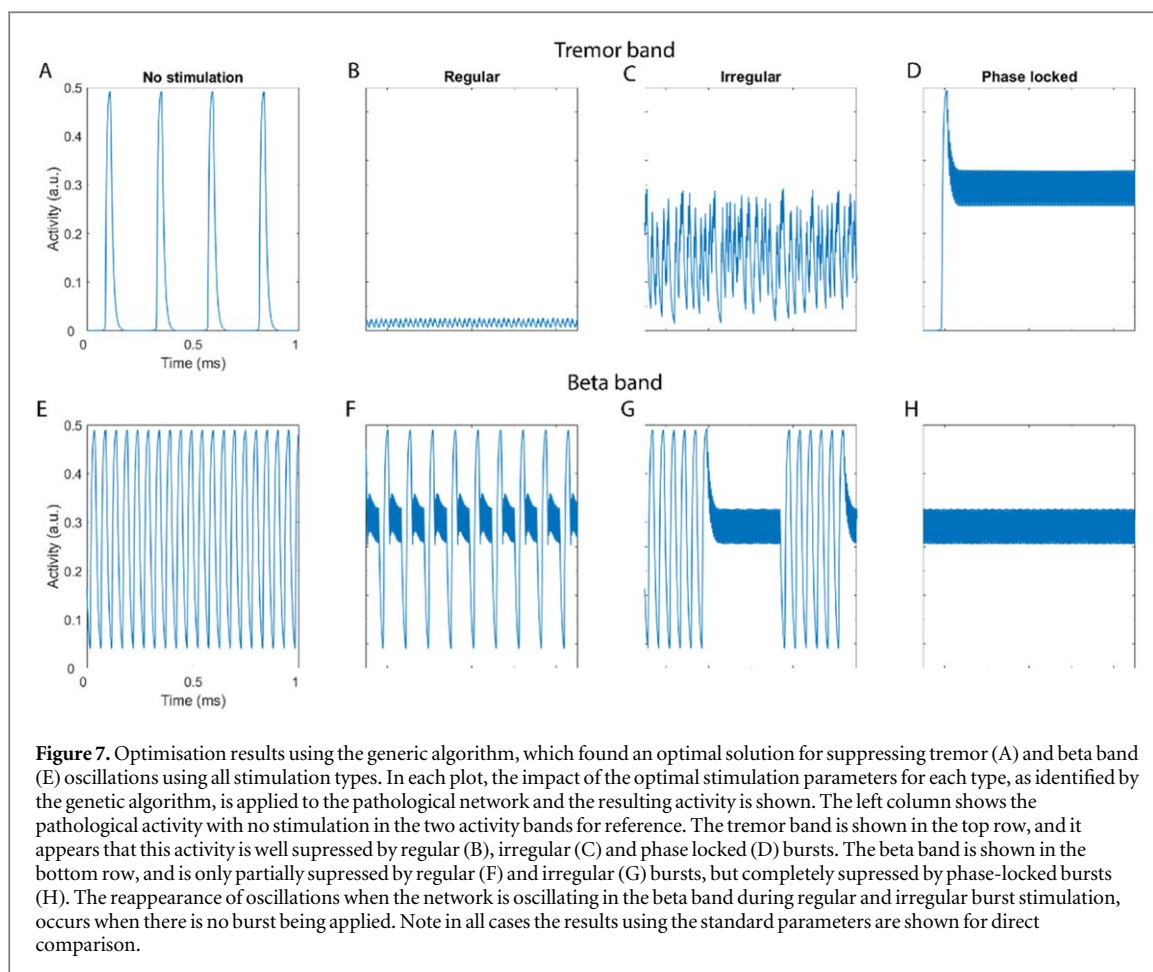


Figure 7. Optimisation results using the generic algorithm, which found an optimal solution for suppressing tremor (A) and beta band (E) oscillations using all stimulation types. In each plot, the impact of the optimal stimulation parameters for each type, as identified by the genetic algorithm, is applied to the pathological network and the resulting activity is shown. The left column shows the pathological activity with no stimulation in the two activity bands for reference. The tremor band is shown in the top row, and it appears that this activity is well suppressed by regular (B), irregular (C) and phase locked (D) bursts. The beta band is shown in the bottom row, and is only partially suppressed by regular (F) and irregular (G) bursts, but completely suppressed by phase-locked bursts (H). The reappearance of oscillations when the network is oscillating in the beta band during regular and irregular burst stimulation, occurs when there is no burst being applied. Note in all cases the results using the standard parameters are shown for direct comparison.

important to note that in their study the model was a detailed biophysical model, and as such the applied DBS (standard or temporally non-regular) could impact on a variety of neural processes, from ion channels, to synapses to networks. In our study, we are considering the effect on one aspect of each disease, i.e. that the brain exhibits oscillations at the tremor/beta band and proposing that clinical improvement is achieved by disrupting such oscillations.

We initially found that in all cases, the beta band network activity was not well suppressed, neither with regular bursts, randomly applied bursts, nor phase-locked bursts. This is striking as the beta band has been suggested to act as a marker for specific symptoms of Parkinson's disease. Furthermore, our previous study showed that the beta band activity was well-suppressed by continuous DBS, although it did require a higher amplitude. Interestingly, in a previous study of phase-locked stimulation the authors also showed the impact of phase locked stimulation on Wilson-Cowan models fitted to patients' tremor data (Duchet *et al* 2020). These results may indicate that the tremor band activity may act as a better marker for pathological activity and improvement with stimulation. Although new work shows that STN DBS can interrupt beta oscillations in the basal ganglia, though in more detailed model (Adam *et al* 2022). We also found that GPe stimulation did not perform as well as STN stimulation, which

could be in contrast with new study about GP being a hub for oscillations (Crompe *et al* 2020). However, future work could consider the role of targeting different regions for different symptoms of disease which are better suppressed by specific burst stimuli.

We went on to perform optimisation of the burst parameters via a genetic algorithm. We allowed the algorithm to find the amplitude, frequency, and duration (which determined both inter-burst frequency and duration of the burst) of the stimulus. The algorithm found an optimal set of parameters for suppressing the tremor band activity via regular, irregular and phase locked bursts of stimulation. Interestingly, the algorithm found a set of parameters for the phase locked bursts which suppressed the beta band activity, but the regular or irregular bursts could only partially suppress the beta band activity. Interestingly, tremor band activity was best suppressed by regular bursts with a high inter-burst frequency and beta band activity was best suppressed by phase-locked bursts with a low inter-burst frequency. This approach was key to showing that such bursts of DBS can suppress both kinds of pathological activity in our network, however, this comes with some limitations.

Furthermore, clinical studies such as Kuncel *et al* (2007), show that amplitude and frequency of DBS are intimately correlated with tremor suppression in participants with ET. They found that at low frequency

DBS had a worsening effect on tremor as the DBS amplitude increased. But at high frequency, there was tremor suppression as the amplitude of DBS increased. This is in line with our results for the tremor band oscillations, but not for the beta band. However, in our study while we varied amplitude and frequency in the optimisation algorithm, future work could explore broader ranges to encompass lower frequency bursts of DBS in line with the Kuncel *et al* study. Interestingly, adaptive DBS approaches which typically use beta power in the STN as a control signal and switches DBS on and off as a threshold is crossed, resembles irregular bursts of DBS (for example Piña-Fuentes *et al* 2020). Compared to our results, this may indicate that longer irregular bursts of DBS would be more effective at suppressing beta. Our optimisation results would support this as the optimal burst durations for suppressing beta were longer than for tremor band oscillations. Strikingly, a very recent clinical trial of adaptive DBS suggests that beta may not in fact be the optimal marker for use as a control signal, but that gamma band oscillations may better encode high/low dopamine states (Oehrns *et al* 2024). This suggests that more understanding of the role of different oscillatory bands with respect to symptoms is needed, and particularly may be necessary in a case-by-case basis.

The permitted range of the parameters could be extended further, to allow the algorithm more possibility of finding the best fit. Furthermore, the burst duration and inter-burst frequency could be uncoupled into two independent parameters which would further allow more exploration of the parameter space. Finally, the model used here is a population approach, which allows exploration of the dynamics of the network structure. The simplicity of this approach, compared to detailed biophysical models incorporating morphological details and multiple ion channels and to simplified biophysical models such as the integrate and fire model, is intentional as our aim is to consider the dynamics of the network without reliance on physiological properties. While our model cannot explore all possible mechanisms of DBS such as neuroprotection (Herrington *et al* 2016), one important concept of DBS as an informational lesion was introduced 20 years ago (Grill, Snyder and Miocinovic 2004). Here, Parkinsonian symptoms are thought to be generated by pathological information being transmitted through the basal ganglia, and DBS acts as an informational lesion, allowing this transmission to be blocked. This theory has gained traction in recent years (Dorval *et al* 2010, McConnell *et al* 2012, Anderson *et al* 2015) and most recently, an experimental study of DBS in mouse hippocampus has shown evidence for stimulation induced membrane potential depolarisation and entrainment at stimulation frequency (Lowet *et al* 2022). Such results are consistent with our modelling results, which show how regular and now bursts of DBS can change network dynamics and future work

could address the limitations of our approach, by making links to single neuron models.

5. Conclusion

In conclusion, our study shows that in a network based computational model, bursts of DBS may provide as good suppression of synchronised activity, as continuous DBS does. In practice, such bursts of activity would provide an improvement for patients as the energy consumption would be decreased, and therefore internal pulse generators would require less charging and surgical replacements. However, we must consider the impact of amplitude as we found an effect of the higher amplitude bursts driving network activity, which was not apparent with continuous DBS.


Data availability statement

All data that support the findings of this study are included within the article (and any supplementary files).

ORCID iDs

Nada Yousif  <https://orcid.org/0000-0001-9769-1837>

Peter G Bain  <https://orcid.org/0000-0002-4678-8417>

Dipankar Nandi  <https://orcid.org/0000-0001-8305-2655>

Roman Borisyuk  <https://orcid.org/0000-0003-1384-9057>

References

- Adam E M *et al* 2022 Deep brain stimulation in the subthalamic nucleus for Parkinson's disease can restore dynamics of striatal networks *PNAS* **119** e2120808119
- van Albada S J *et al* 2009 Mean-field modeling of the basal ganglia-thalamocortical system. II: dynamics of parkinsonian oscillations *J. Theor. Biol.* **257** 664–88
- Anderson C J *et al* 2015 Subthalamic deep brain stimulation reduces pathological information transmission to the thalamus in a rat model of parkinsonism *Frontiers in Neural Circuits* **9** 1–11
- Benabid A L *et al* 1987 Combined (thalamotomy and stimulation) stereotactic surgery of the VIM thalamic nucleus for bilateral Parkinson disease *Applied neurophysiology* **50** 344–6
Available at: <http://ncbi.nlm.nih.gov/pubmed/3329873> (Accessed: 23 August 2017).
- Birdno M J *et al* 2012 Stimulus features underlying reduced tremor suppression with temporally patterned deep brain stimulation *Journal of Neurophysiology* **107** 364–83
- Brocker D T *et al* 2013 Improved efficacy of temporally non-regular deep brain stimulation in Parkinson's disease *Exp. Neurol.* **239** 60–7
- Chu H Y *et al* 2015 Heterosynaptic regulation of external globus pallidus inputs to the subthalamic nucleus by the motor cortex *Neuron* **85** 364–76
- Chu H Y *et al* 2017 Loss of hyperdirect pathway cortico-subthalamic inputs following degeneration of midbrain dopamine neurons *Neuron* **95** 1306–1318.e5
- Crompe B de la *et al* 2020 The globus pallidus orchestrates abnormal network dynamics in a model of Parkinsonism *Nature Communications* **11** 1–14

- Daria Bogdan I *et al* 2020 Optimal parameters of deep brain stimulation in essential tremor: a meta-analysis and novel programming strategy *Journal of Clinical Medicine* **9** 1–13
- Denham M J and Borisyuk R M 2000 A model of theta rhythm production in the septal-hippocampal system and its modulation by ascending brain stem pathways *Hippocampus* **10** 698–716
- Deuschl G, Bain P and Brin M 1998 Consensus statement of the movement disorder society on tremor. Ad Hoc scientific committee *Movement Disorders: Official Journal of the Movement Disorder Society* **13** 2–23 Available at: <http://ncbi.nlm.nih.gov/pubmed/9827589> (Accessed: 29 April 2019).
- Dorval A D *et al* 2010 Deep brain stimulation alleviates parkinsonian bradykinesia by regularizing pallidal activity *Journal of Neurophysiology* **104** 911–21
- Duchet B *et al* 2020 Phase-dependence of response curves to deep brain stimulation and their relationship: from essential tremor patient data to a Wilson–Cowan model *Journal of Mathematical Neuroscience* **10** 4
- Duchet B *et al* 2021 Optimizing deep brain stimulation based on isostable amplitude in essential tremor patient models *J. Neural Eng.* **18** 046023
- Grill W M, Snyder A N and Miocinovic S 2004 Deep brain stimulation creates an informational lesion of the stimulated nucleus *Neuroreport* **15** 1137–40
- Hauptmann C and Tass P A 2007 Therapeutic rewiring by means of desynchronizing brain stimulation *BioSystems* **89** 173–81
- Herrington T M *et al* 2016 Mechanisms of deep brain stimulation *Journal of Neurophysiology* **115** 19–38
- Holt A B *et al* 2016 Phasic burst stimulation: a closed-loop approach to tuning deep brain stimulation parameters for parkinson's disease *PLoS Comput. Biol.* **12** e1005011
- Khaledi-Nasab A, Kromer J A and Tass P A 2021a Long-lasting desynchronization effects of coordinated reset stimulation improved by random jitters *Frontiers in Physiology* **12** 1446
- Khaledi-Nasab A, Kromer J A and Tass P A 2021b Long-lasting desynchronization of plastic neural networks by random reset stimulation *Frontiers in Physiology* **11** 1843
- Koeglsperger T *et al* 2019 Deep brain stimulation programming for movement disorders: current concepts and evidence-based strategies *Frontiers Neurol.* **10** 410
- Kringelbach M L *et al* 2007 Translational principles of deep brain stimulation *Nature reviews. Neuroscience* **8** 623–35
- Kuncel A M and Grill W M 2004 Selection of stimulus parameters for deep brain stimulation *Clinical Neurophysiology* **115** 2431–41
- Kuncel A M, Cooper S E, Wolgamuth B R and Grill W M 2007 Amplitude- and Frequency-Dependent Changes in Neuronal Regularity Parallel Changes in Tremor With Thalamic Deep Brain Stimulation *IEEE Transactions on Neural Systems and Rehabilitation Engineering* **15** 190–197
- Leblois A *et al* 2006 Competition between feedback loops underlies normal and pathological dynamics in the basal ganglia *J. Neurosci.* **26** 3567–83
- Li G *et al* 2021 Multiscale neural modeling of resting-state fMRI reveals executive-limbic malfunction as a core mechanism in major depressive disorder *NeuroImage: Clinical* **31** 102758
- Little S and Brown P 2014 The functional role of beta oscillations in Parkinson's disease *Parkinsonism & Related Disorders* **20** S44–8
- Litvak V *et al* 2011 Resting oscillatory cortico-subthalamic connectivity in patients with Parkinson's disease *Brain* **134** 359–74
- Louis E D and Ferreira J J 2010 How common is the most common adult movement disorder? Update on the worldwide prevalence of essential tremor *Movement Disorders* **25** 534–41
- Lowet E *et al* 2022 Deep brain stimulation creates informational lesion through membrane depolarization in mouse hippocampus *Nat. Commun.* **13** 1–15
- Madadi Asl M *et al* 2022 Inhibitory spike-timing-dependent plasticity can account for pathological strengthening of pallido-subthalamic synapses in parkinson's disease *Frontiers in Physiology* **13** 1–13
- Madadi M *et al* 2023 Decoupling of interacting neuronal populations by time-shifted stimulation through spike-timing-dependent plasticity *PLOS Computational Biology* **19** e1010853
- McConnell G C *et al* 2012 Effective deep brain stimulation suppresses low-frequency network oscillations in the basal ganglia by regularizing neural firing patterns *J. Neurosci.* **32** 15657–68
- McIntyre C C and Hahn P J 2010 Network perspectives on the mechanisms of deep brain stimulation *Neurobiol. Dis.* **38** 329–37
- Merrison-Hort R *et al* 2013 An interactive channel model of the basal ganglia: bifurcation analysis under healthy and parkinsonian conditions *The Journal of Mathematical Neuroscience* **3** 14
- Milardi D *et al* 2019 The cortico-basal ganglia-cerebellar network: past, present and future perspectives *Frontiers in Systems Neuroscience* **13** 61
- Nambu A, Tokuno H and Takada M 2002 Functional significance of the cortico-subthalamo-pallidal 'hyperdirect' pathway *Neurosci. Res.* **43** 111–7
- Oehr C R *et al* 2024 Chronic adaptive deep brain stimulation versus conventional stimulation in Parkinson's disease: a blinded randomized feasibility trial *Nature Medicine [Preprint]* **30** 3345–56
- Oza C S *et al* 2018 Patterned low-frequency deep brain stimulation induces motor deficits and modulates cortex-basal ganglia neural activity in healthy rats *Journal of Neurophysiology* **120** 2410–22
- Pei H *et al* 2024 Deep brain stimulation mechanisms in parkinson's disease: immediate and long-term effects *Journal of Integrative Neuroscience* **23** 114
- Pfeifer K J *et al* 2021 Coordinated reset vibrotactile stimulation induces sustained cumulative benefits in parkinson's disease *Frontiers in Physiology* **12** 200
- Piña-Fuentes D *et al* 2020 Acute effects of adaptive deep brain stimulation in parkinson's disease *Brain Stimulation* **13** 1507–16
- Popovych O V, Hauptmann C and Tass P A 2006 Control of neuronal synchrony by nonlinear delayed feedback *Biol. Cybern.* **95** 69–85
- Potel S R *et al* 2022 Advances in DBS technology and novel applications: focus on movement disorders *Current Neurology and Neuroscience Reports* **22** 577–88
- Rubin J E and Terman D 2004 High frequency stimulation of the subthalamic nucleus eliminates pathological thalamic rhythmicity in a computational model *J. Comput. Neurosci.* **16** 211–35
- Santos-Valencia F *et al* 2019 Temporally irregular electrical stimulation to the epileptogenic focus delays epileptogenesis in rats *Brain Stimulation* **12** 1429–38
- Summerson S R, Aazhang B and Kemere C 2015 Investigating irregularly patterned deep brain stimulation signal design using biophysical models *Frontiers in Computational Neuroscience* **9** 1–10
- Tass P A *et al* 2012 Coordinated reset has sustained aftereffects in Parkinsonian monkeys *Ann. Neurol.* **72** 816–20
- Toth K and Wilson D 2022 Control of coupled neural oscillations using near-periodic inputs *Chaos* **32** 033130
- Tysnes O B and Storstein A 2017 Epidemiology of Parkinson's disease *J. Neural Transm.* **124** 901–5
- Vedam-Mai V *et al* 2021 Proceedings of the eighth annual deep brain stimulation think tank: advances in optogenetics, ethical issues affecting dbs research, neuromodulatory approaches for depression, adaptive neurostimulation, and emerging DBS technologies *Frontiers in Human Neuroscience* **15** 1–24
- Wilson H R and Cowan J D 1972 Excitatory and Inhibitory Interactions in Localized Populations of Model Neurons *Biophys. J.* **12** 1–24
- Yousif N *et al* 2012 Reversing the polarity of bipolar stimulation in deep brain stimulation for essential tremor: a theoretical explanation for a useful clinical intervention *Neurocase* **20** 37–41
- Yousif N *et al* 2017 A network model of local field potential activity in essential tremor and the impact of deep brain stimulation *PLoS Comput. Biol.* **13** e1005326
- Yousif N *et al* 2020 A population model of deep brain stimulation in movement disorders from circuits to cells *Front. Hum. Neurosci.* **14** 2020
- Zeitler M and Tass P A 2018 Computationally developed sham stimulation protocol for multichannel desynchronizing stimulation *Frontiers in Physiology* **9** 512